



## Analysis of fabric evolution and metamorphic reaction progress at Lago della Vecchia-Valle d'Iroga, Sesia-Lanzo Zone, Western Alps

Luca Corti , Gioele Alberelli, Davide Zanoni & Michele Zucali

To cite this article: Luca Corti , Gioele Alberelli, Davide Zanoni & Michele Zucali (2017) Analysis of fabric evolution and metamorphic reaction progress at Lago della Vecchia-Valle d'Iroga, Sesia-Lanzo Zone, Western Alps, Journal of Maps, 13:2, 521-533, DOI: [10.1080/17445647.2017.1331177](https://doi.org/10.1080/17445647.2017.1331177)

To link to this article: <http://dx.doi.org/10.1080/17445647.2017.1331177>



© 2017 The Author(s). Published by Informa UK Limited, trading as Taylor & Francis Group on behalf of Journal of Maps



[View supplementary material](#)



Published online: 15 Jun 2017.



[Submit your article to this journal](#)



Article views: 135



[View related articles](#)



[View Crossmark data](#)



## Analysis of fabric evolution and metamorphic reaction progress at Lago della Vecchia-Valle d'Irona, Sesia-Lanzo Zone, Western Alps

Luca Corti , Gioele Alberelli, Davide Zanoni  and Michele Zucali 

Dipartimento di Scienze della Terra 'A. Desio', Università degli Studi di Milano, Milano, Italy

### ABSTRACT

The Lago della Vecchia-Valle d'Irona rocks are part of the Eclogitic Micaschists Complex (EMC) of the Sesia-Lanzo Zone, western Austroalpine domain. The 1:10,000 scale map includes metaintrusive, minor micaschist, banded gneiss, and metabasic boudins. The multiscale structural analysis reveals successive magmatic and tectono-metamorphic stages: during M0 the metaintrusive protoliths emplaced; D1 took place under eclogite-facies conditions; during D2 stage, a pervasive foliation developed under retrograde blueschist-facies conditions; D3–D4 and D5 structures developed under greenschist-facies conditions; during M6 andesitic dykes intruded. The mapped degree of fabric evolution (FE) and metamorphic transformation (MT) related to D2-foliation shows that the MT was not only controlled by bulk rock and mineral compositions, but also by FE. The development of a pervasive blueschist-facies D2-foliation is in contrast with the eclogitic dominant fabric generally recorded in the EMC. This difference suggests that FE and MT are potentially responsible for km-scale heterogeneities in the tectono-metamorphic record.

### ARTICLE HISTORY

Received 14 December 2016  
Accepted 12 May 2017



### KEYWORDS

Multiscale structural analysis; fabric evolution; metamorphic transformation progress; petro-structural mapping; blueschist-facies condition; Austroalpine

### 1. Introduction

Within convergent margins, the coupling and uncoupling of lithospheric slices are responsible for the tectonic architecture of metamorphic belts (e.g. Spalla, Gosso, Marotta, Zucali, & Salvi, 2010). The lithospheric slices can be recognized as tectono-metamorphic units once their tectonic and metamorphic history is proved homogeneous over a defined time interval (Spalla, Zucali, di Paola, & Gosso, 2005). Petro-structural mapping and multiscale structural analysis are crucial to characterize the tectono-metamorphic evolution of lithospheric slices and the relationships between degree of fabric evolution (FE) and metamorphic transformation (MT). In particular, the relationship between FE and metamorphic reaction progress with the development of dominant (i.e. pervasive) fabric can be used to investigate the complexity of convergent dynamics (e.g. Salvi, Spalla, Zucali, & Gosso, 2010; Gosso et al., 2015). Adjacent rock volumes characterized by the same dominant fabric may record different tectono-metamorphic histories. In contrast, adjacent rock volumes showing dominant fabrics developed under different metamorphic conditions may record the same tectono-metamorphic history due to heterogeneous registration of the superposed deformation and metamorphic stages (Spalla et al., 2005). In order to evaluate whether rock volumes record the same tectono-metamorphic history, mapping petro-structural

heterogeneities in adjacent rock volumes is crucial (e.g. Delleani, Spalla, Castelli, & Gosso, 2012; Delleani, Spalla, Castelli, & Gosso, 2013; Gosso et al., 2015; Salvi et al., 2010; Zucali, Spalla, & Gosso, 2002). Since deformation heterogeneity commonly affects crystalline basements (e.g. Mørk, 1985; Myers, 1970), the field structural correlation exclusively grounded on geometric criteria is not reliable, because of spatial variations in deformation style (Spalla et al., 2010). During incremental deformation related to a specific stage, rock volumes may escape deformation (coronite) or may be partially (tectonite) or pervasively (mylonite) deformed (Lardeaux & Spalla, 1990). In coronitic (low-strain) domains, metamorphic reactions take place without formation of a new oriented fabric. Where the strain is accumulated, tectonic and mylonitic fabric develop in intermediate and high-strain domains, respectively. In the last two cases metamorphic assemblages define normal planar/linear tectonites or mylonites (Gosso et al., 2015; Salvi et al., 2010; Spalla et al., 2010; Zucali et al., 2002). Therefore structural correlation in metamorphic basements has to be based on a coherent sequence of tectono-metamorphic stages. Heterogeneous partitioning of deformation makes this correlation difficult, but allows the preservation of structures and related metamorphic assemblages that can be used to trace back the tectono-metamorphic history (Spalla et al., 2010).

**CONTACT** Luca Corti  [luca.corti@unimi.it](mailto:luca.corti@unimi.it)  Dipartimento di Scienze della Terra 'A. Desio', Università degli Studi di Milano, Via Mangiagalli 34, 20133 Milano, Italy

© 2017 The Author(s). Published by Informa UK Limited, trading as Taylor & Francis Group on behalf of Journal of Maps

This is an Open Access article distributed under the terms of the Creative Commons Attribution-NonCommercial License (<http://creativecommons.org/licenses/by-nc/4.0/>), which permits unrestricted non-commercial use, distribution, and reproduction in any medium, provided the original work is properly cited.

In this work, we combined geological mapping and multiscale structural analysis to produce a petro-structural 1:10,000 scale map of FE and MT and investigate the tectono-metamorphic history of the Eclogitic Micaschists Complex (EMC) at Lago della Vecchia-Valle d'Irona (upper Cervo valley, Biella, Sesia-Lanzo Zone). The study area consists of metaintrusive, minor micaschist, banded gneiss, cataclastic-mylonitic gneiss, and numerous decimeter-sized metabasic boudins and lenses. These rocks preserve Alpine superimposed fabrics that developed under metamorphic conditions varying between eclogite to greenschist facies. The map covers an area of 7.5 km<sup>2</sup> where strain partitioning in metaintrusives led to the preservation of igneous texture and magmatic minerals in coronitic domains wrapped by tectonic and mylonitic foliations. The presented interactive map shows the Alpine superimposed structures and the associated metamorphic assemblages by means of foliation trajectories indicated with different colors (panel 1 and panel 2 of the [Main Map](#)) and the relationships between degree of FE (panel 3 of the [Main Map](#)) and degree of MT (panel 4 of the [Main Map](#)) for the dominant deformational stage. Mineral abbreviations are as in [Kretz \(1983\)](#) with the exception of Wm (white mica), Amp (amphibole), and Op (opaque minerals).

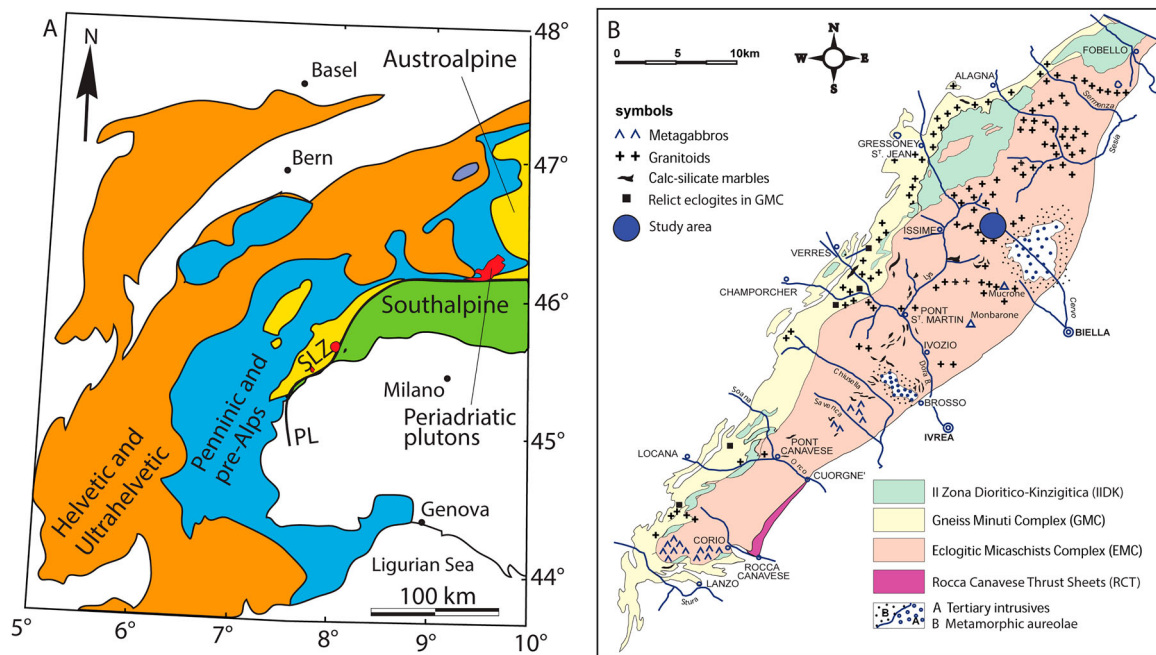
## 2. Geologic outline

The Sesia-Lanzo Zone (SLZ) represents the largest portion (~90 × 20 km) of Austroalpine continental crust that has been eclogitized during the Alpine subduction and now exposed in the axial zone of the Western Alps ([Babist, Handy, Konrad-Schmolke, & Hamerschmidt, 2006](#); [Compagnoni et al., 1977](#); [Dal Piaz, Hunziker, & Martinotti, 1972](#); [Delleani et al., 2013](#); [Lardeaux, 2014](#); [Manzotti, Ballèvre, Zucali, Robyr, & Engi, 2014](#); [Regis et al., 2014](#); [Venturini, Martinotti, Armando, Barbero, & Hunziker, 1994](#); [Zucali et al., 2002](#)). The SLZ is bounded by rocks of the Penninic domain to the northwest, and the Canavese Line (Periadriatic Line (PL)) to the southeast, which separates the SLZ from the Southern Alps ([Figure 1\(A\)](#)).

The SLZ is classically divided into four main complexes ([Figure 1\(B\)](#); [Compagnoni et al., 1977](#); [Gosso, 1977](#)): (1) the II Dioritic-Kinzigitic Zone (IIDK) preserves a pervasive pre-Alpine HT metamorphic imprint; (2) the Gneiss Minuti Complex (GMC) and (3) the EMC display a dominant Alpine metamorphic imprint and locally preserve pre-Alpine HT relicts ([Compagnoni et al., 1977](#); [Gosso, Messiga, Rebay, & Spalla, 2010](#); [Lardeaux, Gosso, Kiénast, & Lombardo, 1982](#); [Manzotti et al., 2014](#); [Zanoni, 2016](#)); (4) the Rocca Canavese Thrust Sheets are characterized by a blueschist Alpine imprint with no eclogite-facies relicts ([Cantù, Spaggiari, Zucali, Zanoni, & Spalla, 2016](#); [Pognante, 1989](#); [Spalla & Zulbati, 2003](#)). The EMC and GMC consist of metapelite,

paragneiss, metagranitoid, metabasite, and impure marble recording Alpine polyphasic deformation and eclogite-facies peak conditions. The peak conditions are represented by the dominant fabric in EMC and by relict domains in GMC ([Pognante, Compagnoni, & Gosso, 1980](#); [Spalla, Lardeaux, Dal Piaz, Gosso, & Messiga, 1996](#); [Spalla et al., 2005](#); [Spalla & Zulbati, 2003](#); [Stünitz, 1991](#); [Tropper & Essene, 2002](#); [Zucali et al., 2002](#)). Eclogite-facies metamorphism is dated around 85–65 Ma ([Cenki-Tok et al., 2011](#); [Regis et al., 2014](#); [Rubatto et al., 2011](#)) and occurred at conditions of 13–20 kbar and 500–600°C ([Compagnoni et al., 1977](#); [Lardeaux & Spalla, 1991](#); [Pognante, Talarico, Rastelli, & Ferrati, 1987](#); [Zucali et al., 2002](#)). Peak conditions were followed by retrogression under blueschist-facies conditions ([Babist et al., 2006](#); [Delleani et al., 2013](#); [Giuntoli & Engi, 2016](#); [Pognante, 1991](#); [Spalla, De Maria, Gosso, Miletto, & Pognante, 1983](#); [Spalla, Lardeaux, Dal Piaz, & Gosso, 1991](#); [Zucali & Spalla, 2011](#)) dated ~60 Ma and occurred at  $P < 15$  kbar and  $T = 450$ – $550$ °C ([Regis et al., 2014](#); [Zucali, 2011](#); [Zucali et al., 2002](#)). Finally, the greenschist re-equilibration occurred at  $P < 8$  kbar and  $T < 350$ °C before 30 Ma ([Babist et al., 2006](#); [Zanoni, Spalla, & Gosso, 2010](#); [Zucali et al., 2002](#)). The exhumation was accomplished during subduction of the Alpine Tethys lithosphere ([Gosso et al., 2010](#); [Polino, Dal Piaz, & Gosso, 1990](#); [Roda, Spalla, & Marotta, 2012](#); [Spalla et al., 1996](#)). Some authors ([Babist et al., 2006](#); [Giuntoli & Engi, 2016](#); [Pognante, 1989](#); [Ramsbotham, Inger, Cliff, Rex, & Barnicoat, 1994](#); [Regis et al., 2014](#); [Venturini, 1995](#)) found evidence of a strong blueschist- to greenschist-facies retrogression within EMC, thus testifying to a heterogeneous record of the tectono-metamorphic stages. On this ground, [Regis et al. \(2014\)](#) interpreted the SLZ as represented by a composite unit that can be divided into several slices with different pre-Mesozoic lithologies and Alpine tectono-metamorphic evolutions: (1) the Druer slice represents the southeastern portion of the SLZ and mainly consists of micaschist and minor metabasite and metagranitoid with a pervasive Alpine eclogite-facies metamorphic imprint; (2) the Intermediate Unit and GMC, in the northwestern portion of SLZ, mainly consist of fine-grained gneiss with dominant retrograde blueschist- to greenschist-facies assemblages; (3) the Fondo slice is a thin and discontinuous layer of Mesozoic metasediment with subordinate metabasite interposed between the Druer slice and GMC-Intermediate Unit. This slice registered two successive Alpine metamorphic imprints under eclogite to blueschist-facies conditions followed by a greenschist-facies overprint; and (4) the IIDK has the characteristics classically described.

The Lago della Vecchia-Valle d'Irona area is located within the EMC ([Figure 1\(B\)](#)), in the Intermediate Unit according to the classification of [Regis et al. \(2014\)](#), just to the north of the Oligocene Biella pluton, far from its contact aureole ([Berger, Thomsen, Ovtcharova, Kapferer, & Mercolli, 2012](#); [Romer,](#)



**Figure 1.** Geological outline of the Sesia-Lanzo Zone. (A) Simplified tectonic map of the Western Alps. SLZ: Sesia-Lanzo Zone. PL: Periadriatic Line (modified from Handy, Babist, Wagner, Rosenberg, & Konrad, 2005). (B) Tectonic map of the Sesia-Lanzo Zone with the location of the study area (modified from Compagnoni et al., 1977; Passchier, Urai, Van Loon, & Williams, 1981; Spalla & Zucali, 2003).

Schärer, & Steck, 1996; Zanoni, 2016; Zanoni, Bado, Spalla, Zucali, & Gosso, 2008).

### 3. Mapping method and analytical techniques

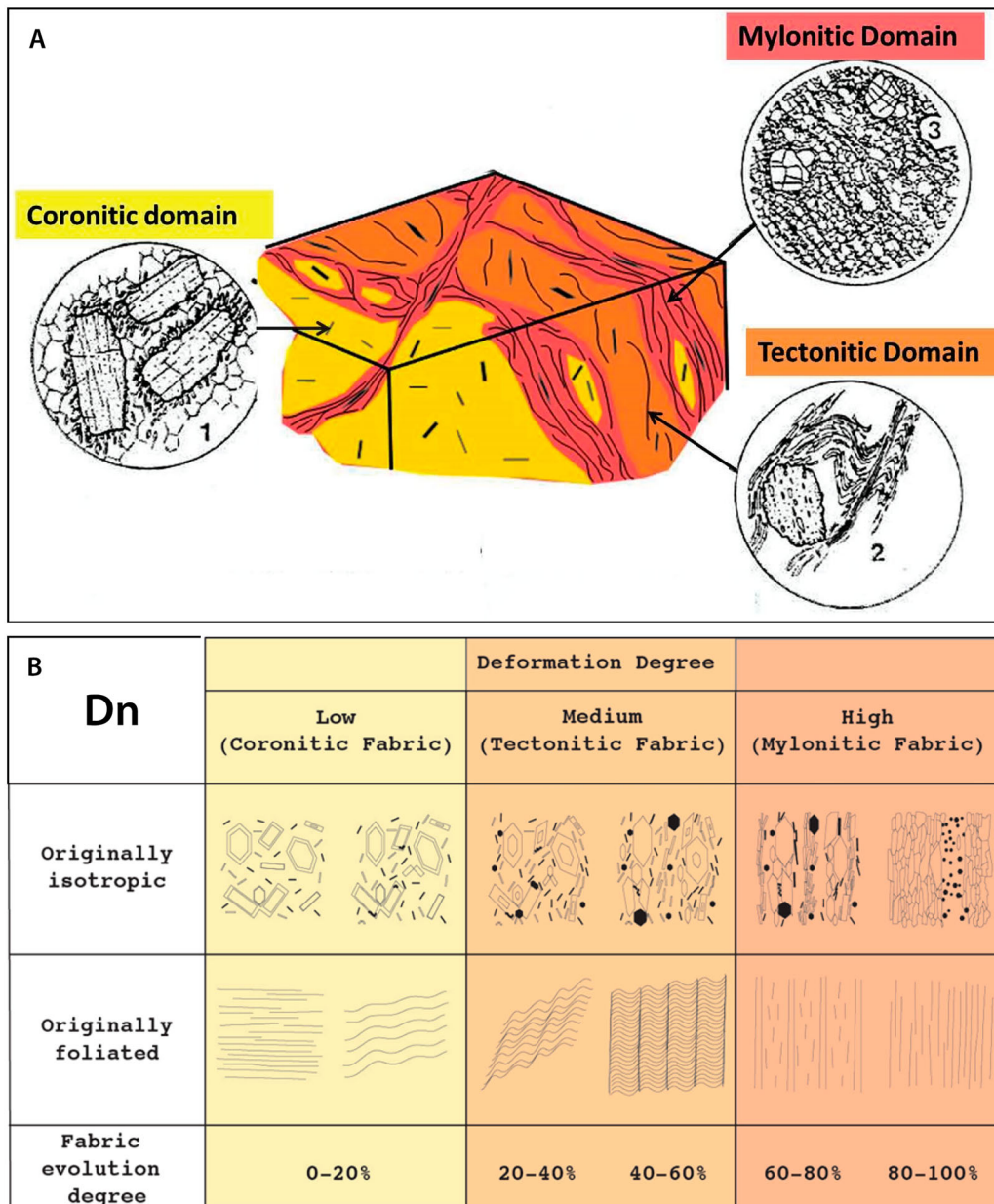
The mapping strategy used here required mesoscale and microscale structural analysis to constrain metamorphic assemblages marking different fabrics and crystallized at different times (Passchier, Myers, & Kroner, 1990; Spalla, Siletto, di Paola, & Gosso, 2000; Zucali et al., 2002). Mesoscale structural analysis aims at recognizing strain gradients, continuously followed in the field, that are classified in terms of coronitic, tectonic, and mylonitic domains (Figure 2(A)).

This analysis is crucial to understand the superposition of tectonic structures that are represented on a structural map by means of form surface trajectories. According to this method, rock types have been represented on an ‘outcrop’ map (panel 1 of the Main Map) in which surfacing rocks are separated by cover drift and for any outcrop the syn-D2 degree of FE is represented. In the ‘interpretative’ map (panel 2 of the Main Map), cover drift is not reported and lithological boundaries are interpreted on the basis of structural data. The two maps, derived from an original mapping at 1:5000 scale, are presented at 1:10,000 scale and show the outcrop contours, lithology, and structural elements that were georeferenced and stored in a Geographic Information System (GIS) geo-database. The topography shape file was acquired from the Geo-Portal of the Piemonte Region (<http://www.geoportale.piemonte.it/>

cms). The orientations of structural elements, such as axial plane foliations, fold axial planes, and axes, are reported on the outcrop map with different symbols to indicate their relative chronology. Two cross-sections and the interpretative map overlay on a digital elevation model (DEM; panel 5 of the Main Map), which is available from the SINAnet (Isprambiente) website (<http://www.sinanet.isprambiente.it/it/sia-ispra/download-mais/dem20/view>), have been performed to show the 3D-geometry of the mapped area. The orientation data are represented on equal area lower hemisphere Schmidt diagrams and grouped according to their relative chronology. The contouring of domains that show homogeneous fabric development is facilitated by integrating meso- with microscale structural analysis to estimate the FE and MT in volume percentage (Figure 2(B); Gosso et al., 2015; Salvi et al., 2010). The estimate of the FE is based on the degree of grain-scale reorganization of the dominant fabrics. The successive stages of crenulation cleavage development up to complete transposition (Bell & Rubenach, 1983; Salvi et al., 2010) were used as a guide. Multiscale deformation partitioning in metaintrusive for the D2 deformational stage is reported as an example in Figure 3. The degree of FE and degree of metamorphic reaction progress are estimated for each deformational stage and rock type. Therefore, for each deformational stage the results are presented in Table 1 and consist of:

- Modal bulk: rock types distinguished based on modal mineral composition and CIPW normative analysis;





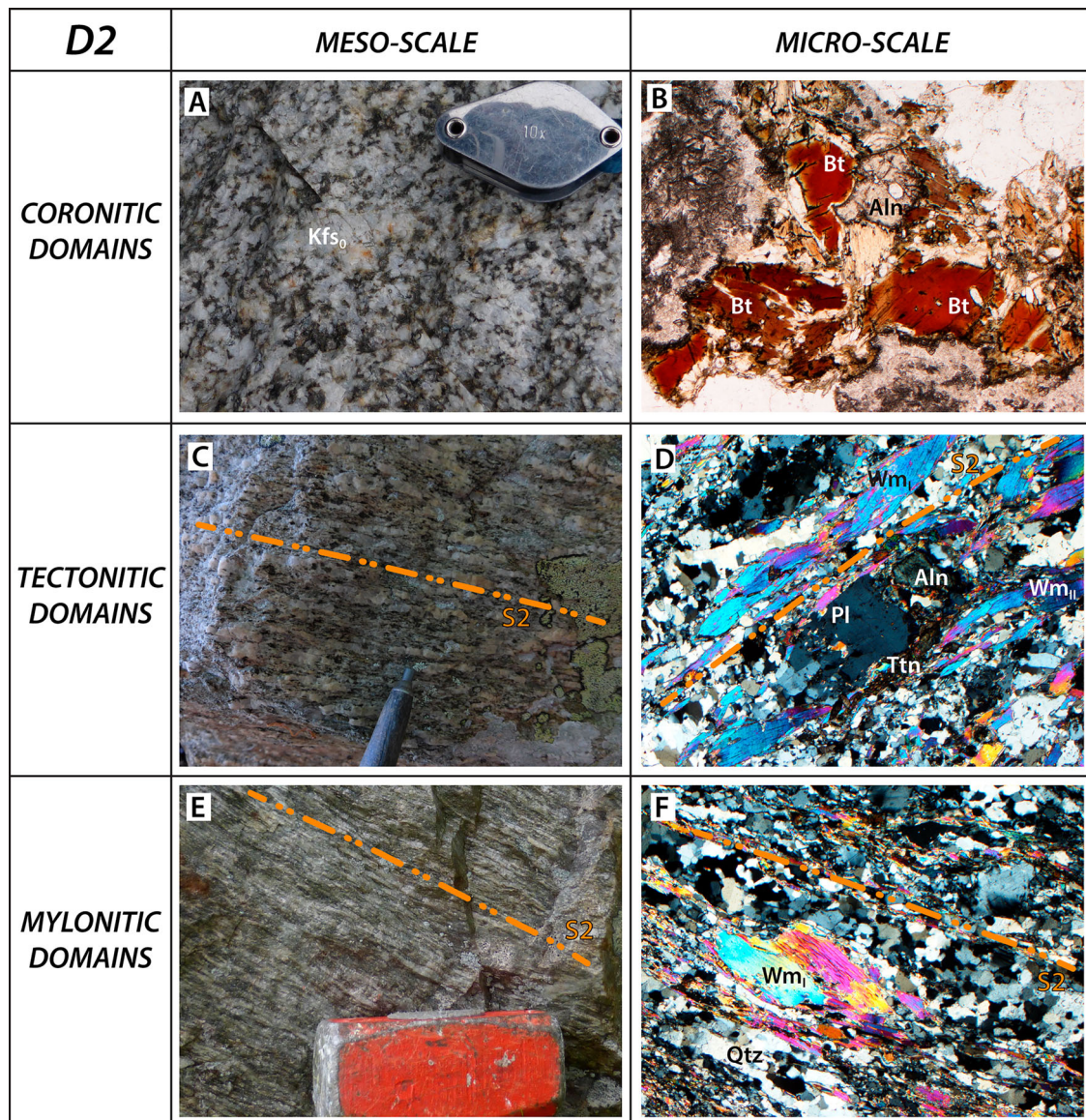
**Figure 2.** (A) Idealized block diagram showing the coexistence of contrasted metamorphic texture due to the deformation partitioning at meso- and micro-scales (modified after Lardeaux & Spalla, 1990). (B) Semi-quantitative estimate of FE during progressive foliation development, starting from originally foliated or isotropic rocks (Bell & Rubenach, 1983; Gosso et al., 2015; Salvi et al., 2010). Dn: successive deformation stage.

- Sample: sample label of analyzed thin section;
- FE: estimation of the area occupied by the orientated planar fabric referred to the deformational stage considered (0–20% coronitic; 21–60% tectonic; and 61–100% mylonitic).
- MT: modal amount of mineral assemblage produced by new mineral growth and recrystallization related to the metamorphic re-equilibration considered (0–100%).

The approach used in this study permitted us to define the pervasiveness of a single deformation-metamorphic stage. Two 1:10,000 thematic maps represent the correlation of FE and MT for D2 stage (panel 3 and panel 4 of the [Main Map](#)).

#### 4. Field data

The mapped area consists of metaintrusives and their country rocks (Zucali, 2011), both characterized by a penetrative foliation marked by Qtz, Wm, Ep, and Grt that wraps metabasite boudins and lenses and micaschist lenses. Based on microstructural analysis, metamorphic assemblages were reconstructed (Table 2). The microstructural and petrographic observations indicate that the pervasive fabric developed at retrograde blueschist-facies conditions and structural relicts of eclogite-facies assemblages are preserved only in the metabasite. Greenschist-facies mineral assemblages are restricted to the main shear zones. Detailed microstructural features of these rock types for each successive deformational stage are displayed in Table 2.



**Figure 3.** Multiscale deformation partitioning (coronitic, tectonic, and mylonitic domains) in metaintrusive for D2 deformational stage. Detailed microstructural descriptions are reported in Table 3. (A) Preserved magmatic fabric and igneous Kfs in low-strain domains (UTM: 415987–5059526). (B) Aggregates of igneous Bt with a brown to reddish brown pleochroism in tabular and pseudo-hexagonal habits and single grains of Aln characterized by high birefringence; plane polarized light (UTM: 417479–5059237). (C) Tectonic domains consist of fine- to medium-grained rocks characterized by the pervasive S2 foliation (UTM: 415394–5058667). (D) S2 is a spaced foliation marked by SPO and LPO of Wm<sub>II</sub> associated with aggregates of Ttn and porphyroblasts of Pl. S2 wraps syn-D1 Wm<sub>I</sub> and magmatic Aln relicts; crossed polars (UTM: 417479–5059237). (E) Mylonitic domains consist of fine-grained rocks with pervasive S2 foliation (UTM: 416299–5059103). (F) S2 is a spaced and discontinuous foliation marked by SPO and LPO of Wm<sub>II</sub> that wraps Wm<sub>I</sub> porphyroblasts; crossed polars (UTM: 415127–5060649).

#### 4.1 Rock types

Metaintrusive is subdivided based on mesoscopic fabric recognized during the fieldwork in: (1) coronitic metaintrusive; (2) tectonic metaintrusive; and (3) mylonitic metaintrusive. The country rocks consist of: (1) tectonic metapelite, with minor eclogitic metabasite boudins; (2) mylonitic- to tectonic-banded gneiss.

##### 4.1.1 Metaintrusive

The intrusive protoliths consist principally of monzogranite that occurs as meter- to decameter-sized outcrops and minor meter-sized granodioritic lenses

within the monzogranite. The partitioning of the Alpine deformation is responsible for the preservation of igneous textures and minerals in meter-sized coronitic lenses and the development of tectonic and mylonitic fabrics in the metaintrusives.

Tectonic and mylonitic foliations wrap coronitic domains, which were found in several localities (Rifugio Lago della Vecchia and to the west of P.ta Canaggio; see the panel 2 of the Main Map) as meter- to decameter-long bodies. Coronitic metaintrusives are medium- to coarse-grained rocks showing a well-preserved isotropic and hypidiomorphic igneous texture with igneous relics such as Bt, Kfs, Pl, Grt, Wm, and Aln, partially replaced



**Table 1.** Evaluation of the degree of FE and degree of metamorphic reaction progress (MT) in metaintrusive for: (A) M0 magmatic stage; (B) D1 deformation stage; (C) D2 deformation stage; and (D) D3–D4 deformation stage.

A M0				B D1			
Modal Bulk	Sample	Igneous Fabric	Magmatic Relicts	Modal Bulk	Sample	FE	MT
		0 - 100%	0 - 100%			0 - 100%	0 - 100%
MO-GR	1.10	100	40	MO-GR	1.10	5	5
	3.10	85	35		3.10	5	5
	3.11B	100	45		3.11B	5	5
	10.3	0	15		10.3	15	10
	10.5	0	15		10.5	25	30
	10.2	0	15		10.2	22	20
GRD	1.1	0	10	GRD	1.1	30	30
	1.2	0	5		1.2	25	25
	1.9	0	10		1.9	35	40
	3.6A	0	5		3.6A	21	25
	5.3	0	5		5.3	25	20
	6.2A	0	5		6.2A	40	25
	3.6B	0	0		3.6B	25	20
	8.1	0	0		8.1	15	10
DR	8.5	0	0	DR	8.5	50	35
	5.6	0	0		5.6	45	30
	6.2B	0	0		6.2B	55	61
	11.2	0	0		11.2	55	65

C D2				D D3-D4			
Modal Bulk	Sample	FE	MT	Modal Bulk	Sample	FE	MT
		0 - 100%	0 - 100%			0 - 100%	0 - 100%
MO-GR	1.10	0	40	MO-GR	1.10	0	10
	3.10	5	45		3.10	20	15
	3.11B	0	35		3.11B	5	10
	10.3	50	30		10.3	64	50
	10.5	40	40		10.5	15	15
	10.2	70	65		10.2	25	20
GRD	1.1	45	45	GRD	1.1	15	15
	1.2	50	60		1.2	10	10
	1.9	55	45		1.9	5	5
	3.6A	63	50		3.6A	10	20
	5.3	55	55		5.3	10	20
	6.2A	60	45		6.2A	20	25
	3.6B	85	75		3.6B	25	30
	8.1	75	70		8.1	15	10
DR	8.5	35	30	DR	8.5	15	10
	5.6	35	40		5.6	45	30
	6.2B	40	50		6.2B	55	35
	11.2	20	25		11.2	15	10

Fabric evolution (FE)			Metamorphic transformation (MT)		
0-20%	21-60%	61-100%	0-20%	21-60%	61-100%

Note: Rock types distinguished on the basis of modal mineral composition and CIPW normative analysis are MO-GR (monzogranite), GRD (granodiorite), and DR (diortite).

by Alpine Grt, Wm, Ep, and Amp (see details in Table 2). Coronitic metaintrusives are constituted by Qtz (30–40%) + Wm (15–20%) + Pl (10–15%) + Grt (10–15%) + Bt (7–10%) + Kfs (5–10%) + Ep (5–10%) + Aln (5%) + Amp (2%).

Tectonic metaintrusives constitutes the most common lithotype in the area and consists of fine- to medium-grained rocks that contain Qtz (30–50%) + Wm (20–30%) + Ep (15–20%) + Grt (5%) + Amp (5%) + magmatic mineral relicts such as Kfs (5%) and Aln (5%). These rocks mostly show a well-developed foliation marked by shape preferred orientation (SPO) of Qtz and aggregates of Wm, Ep, and Grt.

Mylonitic metaintrusives consist of fine-grained rocks showing a millimeter-spaced foliation defined by SPO of Wm, Ep, and Amp that wrap porphyroblasts of Grt and locally magmatic porphyroclasts of Kfs. Mylonitic metaintrusives form decameter- to kilometer-long shear zones mostly trending NW-SE (see the panel 2 and panel 5 within the Main Map) that locally mark the contact between metaintrusive and country rocks. Mylonitic metaintrusives are constituted by Qtz (40–50%) + Wm (15–20%) + Ep (15–20%) + Grt (5–10%) + Amp (5–10%) + Chl (5%). Within the metaintrusives, centimeter- to meter-scale meta-aplitic dykes (type locality: close to Rosei, to the

**Table 2.** Microstructural features of each deformational stage recorded in the mapped rock types.

Stage	Rock type			
	Metaintrusive	Metabasite	Banded gneiss	Metapelite
M0	Preserved M0 fabrics only in coronitic rocks. Igneous mineral relicts are Bt <sub>0</sub> , Kfs <sub>0</sub> , Wm <sub>0</sub> , Aln <sub>0</sub> , Grt <sub>0</sub> , Ttn <sub>0</sub> . Bt <sub>0</sub> occurs in single crystals with a continuous corona of Grt <sub>1</sub> at the contact with Pl <sub>0</sub> . Between single crystals of Wm <sub>0</sub> and Grt <sub>0</sub> , fine-grained corona of Wm <sub>1</sub> , Ep <sub>1</sub> , and Grt <sub>1</sub> developed. Corona of Amp <sub>1</sub> , Grt <sub>1</sub> , and Bt <sub>1</sub> developed between Ttn <sub>0</sub> and Plg <sub>0</sub> . Aln <sub>0</sub> occurs in well-preserved single crystals and different coronitic mineral assemblages developed as a function of the mineral phase Aln <sub>0</sub> is in contact with.	Not found	Pre-D1 fabrics are not preserved. Igneous mineral relicts are found and mainly consist of Kfs <sub>0</sub> crystals partially replaced by P <sub>11</sub> ; within microlithons, sub-millimetre sized Aln <sub>0</sub> crystals are rimmed by coronae of Zo <sub>1</sub> , Czo <sub>1</sub> , and Ep <sub>1</sub> .	Not found
D1	Mineral assemblage: Wm <sub>1</sub> , Czo <sub>1</sub> , Grt <sub>1</sub> , Zo <sub>1</sub> , Qtz <sub>1</sub> , Mnz <sub>1</sub> , and Rt <sub>1</sub> . D1 mineral relicts are preserved as porphyroblasts wrapped by S2-foliation. Grt <sub>1</sub> porphyroblasts show an internal foliation marked by fine-grained crystals of Wm <sub>1</sub> , Zo <sub>1</sub> /Czo <sub>1</sub> , and Rt <sub>1</sub> smaller than in matrix minerals; this suggests that Grt <sub>1</sub> growth started during an earlier stage of S1 development.	Mineral assemblage: Cpx <sub>1</sub> , Wm <sub>1</sub> , Grt <sub>1</sub> , Czo <sub>1</sub> . These minerals are arranged in SPO of Cpx <sub>1</sub> in equilibrium with Grt <sub>1</sub> , Wm <sub>1</sub> , and minor Czo <sub>1</sub> . Cpx <sub>1</sub> occurs as large porphyroblasts with rational grain boundaries with Wm <sub>1</sub> and Grt <sub>1</sub> .	Relicts of D1 fabrics are constituted by Wm <sub>1</sub> , Grt <sub>1</sub> , Ep <sub>1</sub> , Zo <sub>1</sub> /Czo <sub>1</sub> , and Rt <sub>1</sub> . This mineral assemblage consists of large and deformed Wm <sub>1</sub> porphyroblasts, Grt <sub>1</sub> cores with inclusions of Rt <sub>1</sub> , and Zo <sub>1</sub> /Czo <sub>1</sub> boudinated crystals.	Mineral assemblage: Wm <sub>1</sub> , Grt <sub>1</sub> , Zo <sub>1</sub> /Czo <sub>1</sub> , Rt <sub>1</sub> . Relicts of S1 foliation, constituted by SPO of Wm <sub>1</sub> and Zo <sub>1</sub> /Czo <sub>1</sub> , are preserved within microlithons. Grt <sub>1</sub> porphyroblasts show an internal foliation marked by fine-grained crystals of Wm <sub>1</sub> , Zo <sub>1</sub> , and Rt <sub>1</sub> smaller than in the matrix; this suggests that Grt <sub>1</sub> growth started during an earlier stage of S1 development.
D2	Mineral assemblage: Wm <sub>11</sub> , Qtz <sub>11</sub> , Czo <sub>11</sub> , Zo <sub>11</sub> , Grt <sub>11</sub> , P <sub>11</sub> , Ttn <sub>11</sub> , Op <sub>11</sub> . These minerals are arranged in S2 spaced and discontinuous foliation marked by SPO of Wm <sub>11</sub> , Czo <sub>11</sub> , Zo <sub>11</sub> , P <sub>11</sub> , associated with Grt <sub>11</sub> and Ttn <sub>11</sub> . Rational grain boundaries between Grt <sub>11</sub> and S2 marking minerals are preserved in portions where successive fabric overprints are not pervasive. Ttn <sub>11</sub> occurs in small sub-euhedral and euhedral crystals in contact with Wm <sub>11</sub> . S2 is locally associated with boudinage of Zo <sub>1</sub> and gentle folding of Wm <sub>1</sub> .	Mineral assemblage: Cpx <sub>11</sub> , Amp <sub>11</sub> , Wm <sub>11</sub> , Grt <sub>11</sub> , Zo <sub>11</sub> , P <sub>11</sub> , Op <sub>11</sub> . S2 is mainly a discontinuous and spaced foliation that is continuous in high-strain domains. SPO and LPO of Cpx <sub>11</sub> , Amp <sub>11</sub> , Wm <sub>11</sub> , Zo <sub>11</sub> , Czo <sub>11</sub> mark S2 in equilibrium with Grt <sub>11</sub> . D2 phases are also associated with boudinage of Cpx <sub>1</sub> . In low-strain domains the same minerals replace D1 assemblage in coronitic fabrics.	Mineral assemblage: Wm <sub>11</sub> , Grt <sub>11</sub> , Zo <sub>11</sub> /Czo <sub>11</sub> , Ep <sub>11</sub> , Ttn <sub>11</sub> , Qtz <sub>11</sub> . These phases are arranged into a S2 spaced foliation marked by SPO and LPO of Wm <sub>11</sub> , SPO of Zo <sub>11</sub> /Czo <sub>11</sub> and Ep <sub>11</sub> associated with Grt <sub>11</sub> and Ttn <sub>11</sub> . Grains boundaries between Grt <sub>11</sub> and S2 marking minerals are rational in portions where successive fabric overprints are not pervasive. Ttn <sub>11</sub> occurs in small sub-euhedral and euhedral crystals in equilibrium with Wm <sub>11</sub> ; in low-strain domains Ttn <sub>11</sub> defined coronae around Wm <sub>1</sub> and Rt <sub>1</sub> . S2 overprints S1 foliation and is locally associated with boudinage of Zo <sub>1</sub> and Wm <sub>1</sub> .	Mineral assemblage: Wm <sub>11</sub> , Grt <sub>11</sub> , Zo <sub>11</sub> /Czo <sub>11</sub> , Ep <sub>11</sub> , Ttn <sub>11</sub> , Qtz <sub>11</sub> . S2 foliation is a zonal and continuous foliation marked by SPO and LPO of Wm <sub>11</sub> , SPO of Zo <sub>11</sub> /Czo <sub>11</sub> associated with Grt <sub>11</sub> and Ttn <sub>11</sub> .
D3-D4	Mineral assemblage: Wm <sub>111</sub> , Qtz <sub>111</sub> , Ep <sub>111</sub> , P <sub>111</sub> , Ttn <sub>111</sub> , Ch <sub>111</sub> , Amp <sub>111</sub> , Op <sub>111</sub> . D3-D4 are characterized by local development, at low angle with S2 foliation, of S3 foliation marked by fine-grained SPO of Wm <sub>111</sub> , Ep <sub>111</sub> , Amp <sub>111</sub> , and Ch <sub>111</sub> . In low-strain domains, the same minerals replace previous assemblages.	Mineral assemblage: Wm <sub>111</sub> , Amp <sub>111</sub> , Ep <sub>111</sub> , P <sub>111</sub> , Ttn <sub>111</sub> , Qtz <sub>111</sub> , Op <sub>111</sub> . D3-D4 are constituted by fine-grained aggregate of Amp <sub>111</sub> , Ep <sub>111</sub> , Wm <sub>111</sub> , Ttn <sub>111</sub> showing SPO between boudinated Cpx and along grain boundary of porphyroblasts.	Mineral assemblage: Wm <sub>111</sub> , Ep <sub>111</sub> , Ch <sub>111</sub> , Amp <sub>111</sub> , P <sub>111</sub> , Qtz <sub>111</sub> . D3-D4 are characterized by local development of S3 foliation at low angle with S2 foliation. S3 is marked by fine-grained aggregates of Wm <sub>111</sub> , Ep <sub>111</sub> , Ch <sub>111</sub> , Amp <sub>111</sub> . In low-strain domains, the same minerals replace previous assemblages. Wm <sub>111</sub> and Ch <sub>111</sub> developed along [001] planes of kinked Wm <sub>111</sub> ; Ch <sub>111</sub> partially replaces Grt <sub>111</sub> along grain boundaries and micro-fractures. Zo <sub>111</sub> and Ep <sub>111</sub> are overgrown by a fine-grained aggregate of Wm <sub>111</sub> and Ep <sub>111</sub> .	Mineral assemblage: Wm <sub>111</sub> , Ep <sub>111</sub> , Ch <sub>111</sub> , Amp <sub>111</sub> , P <sub>111</sub> , Qtz <sub>111</sub> . D3-D4 are characterized by micro-folding associated with an axial plane S3 foliation marked by fine-grained aggregates of Wm <sub>111</sub> , Ep <sub>111</sub> , Ch <sub>111</sub> , and Amp <sub>111</sub> . In low-strain domains, the same minerals replace previous assemblages. Wm <sub>111</sub> and Ch <sub>111</sub> developed along [001] planes of kinked Wm <sub>111</sub> ; Ch <sub>111</sub> partially replaces Grt <sub>111</sub> along grain boundaries and micro-fractures.
D5	Mineral assemblage: Ch <sub>111</sub> , Amp <sub>111</sub> , Qtz <sub>111</sub> , Op <sub>111</sub> . D5 is characterized by the development of coronitic mineral assemblage marked by Ch <sub>111</sub> and Amp <sub>111</sub> and it is related to an extremely localized overprint along D5 shear zones.	Not found	Mineral assemblage: Ch <sub>111</sub> , Amp <sub>111</sub> , Qtz <sub>111</sub> , Op <sub>111</sub> . D5 is related to an extremely localized overprint constituted by the development of S5 foliation marked by SPO and LPO of Ch <sub>111</sub> and Amp <sub>111</sub> .	Not found



east of Olmo, located along the Torrente Irogna, and at Colle della Vecchia) and numerous boudins occur.

#### 4.1.2 Banded gneiss

Banded gneiss has intermediate composition between metaintrusive and metapelite and consists of fine-grained rocks. These rocks show a centimeter- to meter-thick layering of leucocratic Wm-poor and mafic Wm-Ep rich layers. The layering seems to be related to the degree of FE; the layering thickness decreases with the increase of the finite strain, as it occurs near Irogna Inferiore. Banded gneiss mostly outcrops between mylonitic and tectonic metaintrusive and metapelite lenses (see the [Main Map](#)).

In banded gneiss, the pervasive millimeter-spaced foliation is mostly mylonitic and marked by compositional layering. The mafic layers are constituted by Wm (30–45%) + Qtz (10–20%) + Ep (5–15%) + Grt (10–25%) + Amp (5–10%). The contents of Wm, Ep, and Grt highly vary in volume percent as a function of the bulk composition. The leucocratic layers are characterized by a less-developed foliation and are constituted by Qtz (50–60%) + Grt (10–15%) + Pl (10–15%) + Ep (5%) + Wm (5%) + Amp (5%) + probably magmatic relicts of Kfs (< 5%).

#### 4.1.3 Metapelite

The metapelite consists mostly of tectonic micaschist with minor gneiss and occurs as decameter- to meter-sized lenses within the metaintrusive. Metapelite is wrapped and elongated within the pervasive D2-foliation and enclosed in mylonitic metaintrusive and banded gneiss. These rocks mostly outcrop on the west shore of Lago della Vecchia, at Lago del Giaspret, and around C.le d'Irogna. The micaschist consists of fine-grained rocks with a pervasive millimeter-spaced foliation marked by SPO of Wm and Grt. Micaschist is constituted by Wm (15–40%) + Qtz (15–50%) + Grt (15%) + Ep (5–10%) + Amp (5–10%). Metapelite outcropping nearby Lago del Giaspret (see the [Main Map](#)) contains meter-sized metabasic boudins. Micaschist is alternated with fine-grained leucocratic Qtz-rich gneiss in which the pervasive gneissic foliation is marked by Wm, Grt, and Ep. Leucocratic gneiss is constituted by Qtz (50%) + Grt (10–20%) + Wm (10–15%) + Ep (5–10%) + Amp (5%).

#### 4.1.4 Metabasite

Metabasite occurs as meter- to decameter-sized lenses and as centimeter-sized boudins within metaintrusive, banded gneiss, and metapelite. The metabasite is characterized by a foliation marked by SPO of Cpx, Grt, and Wm, which locally is overprinted by the successive structural and metamorphic re-equilibrations.

#### 4.1.5 Gneiss

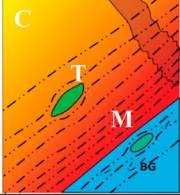
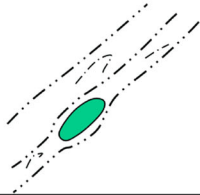
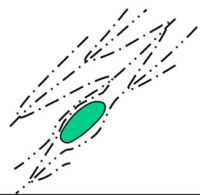
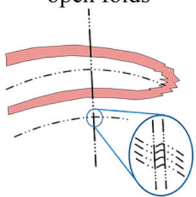
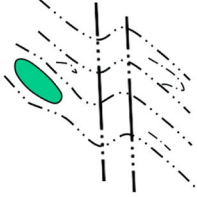

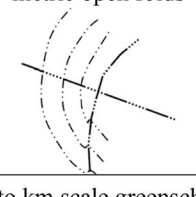
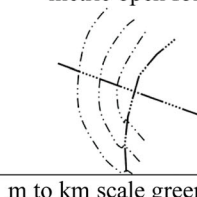
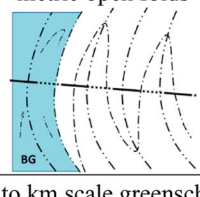
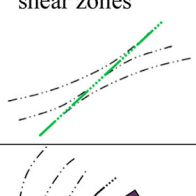
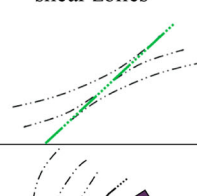


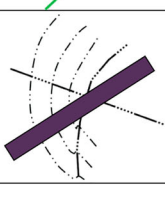
Gneiss outcrops as fine-grained and meter- to decameter-thick rocks displaying a mylonitic contact with all the previous rock types. Gneiss is characterized by cataclastic-mylonitic fabric. Chl + Amp + Qtz + Op constitute the mylonitic millimeter-spaced foliation that transposed and obliterated all previous structures and lithologies.


### 4.2 Structural analysis


The panels 1 and 2 of the [Main Map](#) show the location of the different strain domains for each rock type. In particular, they show coronitic domains wrapped by a network of superposed tectonic foliations and mylonitic shear zones related to successive deformational stages. The identified mineral assemblages ([Table 2](#)) linked to the successive deformational stages ([Table 3](#)) allow definition of the tectono-metamorphic history. Two groups of magmatic (M0, M6) structures and five groups of superposed tectonic structures (D1–D5) are defined. Numbers associated with magmatic and tectonic structures refer to relative chronology. M0 stage consists of undeformed, most probably pre-Alpine, igneous intrusion ([Zucali, 2011](#)). D1–D5 structures consist of fold systems, foliations, and shear zones that are comparable, in terms of their structural features and relative chronology, to the Alpine structures described by [Zucali et al. \(2002\)](#) and [Delleani et al. \(2012\)](#) in the nearby area of M. Mucrone. M6 stage is represented by andesite dyke intrusion that is quite common in the area and dated at the Oligocene (e.g. [Kapferer, Mercolli, Berger, Ovtcharova, & Fügenschuh, 2012](#)). [Table 3](#) is a schematic representation of deformation timing and related pre-Alpine and Alpine mesostructures developed in metaintrusive, banded gneiss, and metapelite. The orientations of fabric elements are summarized in the structural data section of the [Main Map](#). The relationships between the superimposed fabrics and mineral assemblages ([Table 2](#)) recognized at the multiscale have been used to reconstruct the following structural history.


**M0.** Isotropic textures are preserved in meter- to decameter-sized coronitic metaintrusive domains. Coronitic metaintrusive (at Rifugio Lago della Vecchia and west of P.ta Canaggio) preserves Bt<sub>0</sub> ([Figure 4\(A\)](#)), Kfs<sub>0</sub>, euhedral to subeuhedral Pl<sub>0</sub> grains, and interstitial Qtz. In the tectonic and mylonitic domains, the magmatic textures are strongly deformed and the amount of igneous mineral relicts is lower than in the coronitic metaintrusives. Primary magmatic contacts between granitoid and country rocks were not found. Metaintrusives are separated by metapelite by progressively high-strain mylonitic domains that consist of banded gneiss and/or mylonitic metaintrusives themselves (east of Lago del Giaspret, SE of Rifugio della Vecchia, and ESE of Irogna). Aplite dykes intersect igneous fabric and mineral relicts in metaintrusive coronitic


**Table 3.** Schematic representation of mesostructures developed in metaintrusive, banded gneiss, and metapelite during the pre-Alpine and Alpine evolution.


		Metaintrusive	Banded gneiss	Metapelite
Deformation stage	<b>M0</b>	Igneous Textures	Not Found	Not Found
	<b>D1</b>	Not Found	Not Found	S1
	<b>D2</b>			
	<b>D3</b>	cm-sized crenulation and open folds 	cm-sized shear zones 	cm-sized shear zones 
	<b>D4</b>	metric open folds 	metric open folds 	metric open folds 
	<b>D5</b>	m to km scale greenschist shear zones 	m to km scale greenschist shear zones 	m to km scale greenschist shear zones 
	<b>M6</b>			No andesitic dykes cut metapelite


 Andesitic dykes


 Meta-aplite

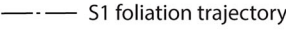
 Coronitic metaintrusive

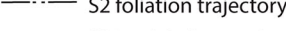
 Tectonic metaintrusive

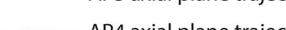
 Mylonitic metaintrusive


 Banded gneiss


 Boudins

 S1 foliation trajectory

 S2 foliation trajectory

 AP3 axial plane trajectory

 AP4 axial plane trajectory

 S5 foliation trajectory

Note: BG: banded gneiss; C: coronitic domains; T: tectonic domains; and M: mylonitic domains.

domains and are overprinted by Alpine foliations in tectonic domains. In this last case, the igneous contact between aplite and metaintrusive is intersected at high angle by the Alpine foliations (Figure 4(B)).

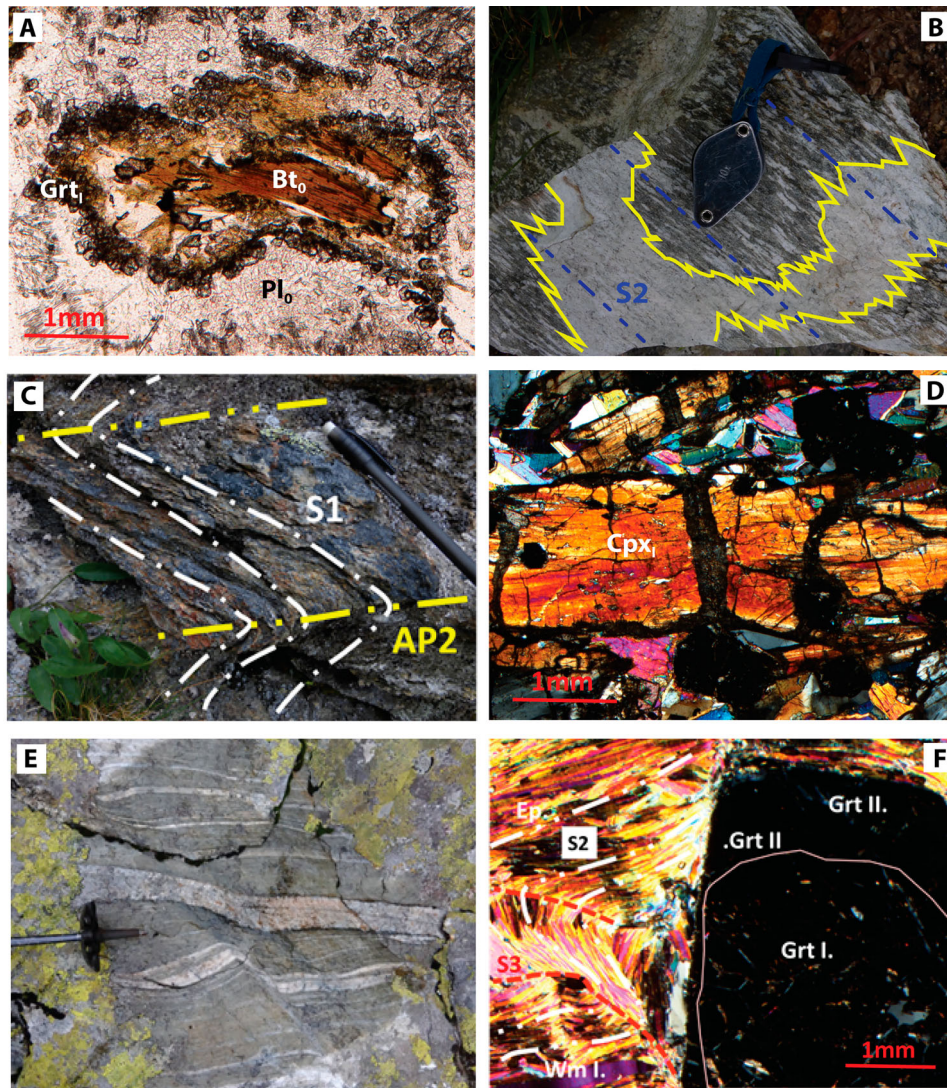
**D1.** During D1 a well-preserved foliation (Figure 4 (C)) developed within tectonic micaschist (S1) nearby Colle d'Iroigna (see the Main Map) with dip azimuth clustering between 320° and 140° and dip varying from 25° to 55°. Relicts of S1 foliation also occur in metabasite boudins (Figure 4(D)).

**D2.** During D2 stage a pervasive S2 foliation developed and previous structures, such as igneous

structures, lithological surfaces, and S1 foliation were parallelized and often transposed into S2. S2 is characterized by 15–50° dip and dip azimuth varying from 90° to 320°, with cluster at a dip azimuth of 125° and dip of 42°. In the micaschists S2, also occurs as axial plane foliation of isoclinal to tight folds (SW-shore of Lago della Vecchia, east of Lago del Giaspret, and north of Colle d'Iroigna; see the panel 2 of the Main Map).

Metaintrusives record the maximum variability of syn-D2 fabric types (coronite to mylonite). In tectonic-mylonitic domains, the S2-foliation wraps around





**Figure 4.** Multiscale structures. (A) Coronitic metaintrusive shows magmatic  $Bt_0$  in single crystals rimmed by a continuous corona of  $Grt_1$  at the contact with magmatic  $Pl_0$ ; plane polarized light (UTM: 417479–5059237). (B) Meta-aplite in tectonic metaintrusive with boundaries deformed and stretched into parallelism with the  $S_2$  penetrative foliation (UTM: 415922–5059543). (C) Tectonic metapelite with  $S_1$  foliation crenulated by  $D_2$  folding (UTM: 415716–5058620). (D) Relicts of  $S_1$  foliation marked by  $Cpx_1$  in metabasic boudin; crossed polars (UTM: 415731–5060114). (E) Mylonitic banded gneiss characterized by layering of  $Wm$ - $Ep$ -bearing layers and a minor leucocratic layers, overprinted by successive  $D_3$  shear zones (UTM: 416241–5058630). (F) Tectonic metapelite shows millimeter-sized porphyroblasts of  $Grt$  displaying a  $Grt_1$  core rich in  $Wm$  and  $Zo$  inclusions surrounded by  $Grt_2$  inclusion free in equilibrium with  $Wm_2$ .  $S_2$  foliation (white dashed line) is marked by  $Wm_2$ ,  $Ep_1$  and  $Ttn_2$ ;  $S_2$  is crenulated during  $S_3$  foliation (red line) development.  $S_3$  is marked by fine-grained crystals of  $Wm_3$ ,  $Ep_3$ , and  $Ch_1$ ; crossed polars (UTM: 416617–5057989).

coronitic domains and elongated metabasic boudins (e.g. toward SE of Lago del Giaspret; see the panel 2 of the [Main Map](#)) and overprints aplitic dykes.  $D_2$  is also responsible for the layering of the banded gneiss being parallel to the  $S_2$  foliation (Figure 4(E)).

**D3.** This deformational stage mainly produced open folds characterized by sub-vertical SE dipping axial planes that affected all lithological boundaries. Generally,  $D_3$  folding is not associated with the development of a new pervasive foliation, however a differentiated  $S_3$  axial plane foliation is developed locally in metaintrusive and banded gneiss (at the top of Valle d'Irogna and between the Rifugio Lago della Vecchia and C.le della Vecchia; see the panel 2 of the [Main Map](#)), within 1–2 cm thick localized shear zones at high angle with the  $S_2$  foliation (Figure 4(F)).

**D4.**  $D_4$  produced open folds (NW of Olmo and north of C.le d'Irogna; see the panel 2 of [Main Map](#)), characterized by a W-dipping sub-horizontal axial plane in micaschists and tectonic metaintrusives. These folds are poorly recorded and are not associated with a new foliation.

**D5.** These structures are related to the development of ductile-brittle meter- to kilometer-long and meter-thick NE-SW trending shear zones. Within these shear zones, mylonitic fabrics are marked by greenschist-facies minerals (see the panel 1 and 2 within the [Main Map](#)). These shear zones ubiquitously affect the contacts between the metaintrusive and banded gneiss (see the panel 2 and panel 5 within the [Main Map](#)).

**M6.** This stage consists of andesitic dykes' intrusion. Sub-vertical andesitic dykes are 0.5–2 meter thick and



trend WNW-ESE. They crosscut all rock types and foliations (several outcrops between the Lago del Giaspret and C.le Irogna; NW of Olmo, along the Torrente Irogna; see the panel 1 of the [Main Map](#)). Only the relationship with the D5 shear zones was not observed.

## 5. Conclusion

The analysis carried out on these metamorphic rocks show that the progress of MTs was controlled by bulk rock, mineral compositions, but it was mainly affected by FE. The maps of degree of FE and MT support this conclusion showing that FE (panel 3 of the [Main Map](#)) and MT (panel 4 of the [Main Map](#)) are strictly correlated regardless of rock types. Moreover, the dominant tectono-metamorphic imprint is related to the D2 stage that is characterized by the highest degree of FE and MT.

Our observation agrees with results obtained in other portions of the subducted continental crust of the Western and Central Alps. For instance, in the nearby area of M. Mucrone the correlation between FE and MT shows that the dominant tectono-metamorphic imprint is related to high degree of FE and MT (Delleani et al., 2012; Delleani et al., 2013; Zucali et al., 2002). Similar results have been also obtained in the Mont Morion complex of the Dent Blanche nappe (Roda & Zucali, 2008) and in the Languard-Tonale unit in the central Austroalpine domain (Salvi et al., 2010). In this last example, the application of this method results in a 3D model of the relationships between FE and MT and the estimation of the volumes affected by textural reworking during polyphase pre-Alpine and Alpine deformations.

In the area mapped in this work, the D2 event is more pervasive with respect to D1 and D3–D4 and S2 foliation displays the highest degree of FE and MT. In all rock types, blueschist-facies mineral assemblages (Table 3) define S2. This finding is in contrast with the nearby metaintrusive of M. Mucrone, where eclogitic mineral assemblages mark the pervasive fabric (Delleani et al., 2012; Delleani et al., 2013; Zucali et al., 2002). Thus, different FE and MT would have affected the retrograde blueschist re-equilibration and potentially generated km-scale heterogeneities within the EMC.

## Software

The geological map, thematic maps, cross-sections, and 3D-model were drawn using Esri ArcMap 10.2.2, Adobe Illustrator CS6, and Move 2016.2. The [Main Map](#) was built using Adobe Illustrator CS6 and Adobe Acrobat X Pro. Photos and diagrams were edited using Adobe Illustrator CS6. Stereoplots were produced with Stereonet 9 (Allmendinger, 2016).

## Acknowledgements

Insightful reviews by Manuel Roda and an anonymous fellow helped us to clarify the ideas presented in the text and map panels. Steven Bernard provided useful advices on map plate layout. Mr. Rizzetti facilitated the use of La Scala shepherd hut during fieldwork.

## Disclosure statement

No potential conflict of interest was reported by the authors.

## Funding

Funding from MIUR (Ministero dell'Istruzione, dell'Università e della Ricerca) PRIN 2010-2011 [grant number 2010AZR98L 'Birth and death of oceanic basins:geodynamic processes from rifting to continental collision in Mediterranean and circum-Mediterranean orogens'] and Linea B del Piano di potenziamento della ricerca Università di Milano ['Analisi delle relazioni deformazione / metamorfismo e deformazione magmatismo applicata all'evoluzione degli orogeni collisionali'].

## ORCID

Luca Corti  <http://orcid.org/0000-0003-0523-6891>

Davide Zanoni  <http://orcid.org/0000-0003-1404-4824>

Michele Zucali  <http://orcid.org/0000-0003-3600-7856>

## References

- Allmendinger, R. (2016). *Stereonet 9 for Windows [Online]*. Retrieved December 14, 2016, from <http://www.geo.cornell.edu/geology/faculty/RWA/programs/stereonet.html>
- Babist, J., Handy, M. R., Konrad-Schmolke, M., & Hammerschmidt, K. (2006). Precollisional, multistage exhumation of subducted continental crust: The Sesia Zone, Western Alps. *Tectonics*, 25, TC6008. doi:10.1029/2005TC001927
- Bell, T. H., & Rubenach, M. J. (1983). Sequential porphyroblast growth and crenulation cleavage development during progressive deformation. *Tectonophysics*, 92, 171–194.
- Berger, A., Thomsen, T. B., Ovtcharova, M., Kapferer, N., & Mercolli, I. (2012). Dating emplacement and evolution of the orogenic magmatism in the internal Western Alps: 1. The Miagliano Pluton. *Swiss Journal of Geosciences*, 105, 49–65. doi:10.1007/s00015-012-0091-7
- Cantù, M., Spaggiari, L., Zucali, M., Zanoni, D., & Spalla, M. I. (2016). Structural analysis of a subduction-related contact in southern Sesia-Lanzo Zone (Austroalpine domain, Italian Western Alps). *Journal of Maps*, 12(1), 22–35. doi:10.1080/17445647.2016.1155925
- Centi-Tok, B., Oliot, E., Rubatto, D., Berger, A., Engi, M., & Janots, E. (2011). Preservation of Permian allanite within an Alpine eclogite facies shear zone at Mt Mucrone, Italy: Mechanical and chemical behavior of allanite during mylonitization. *Lithos*, 125, 40–50. doi:10.1016/j.lithos.2011.01.005
- Compagnoni, R., Dal Piaz, G. V., Hunziker, J. C., Gosso, G., Lombardo, B., & Williams, P. F. (1977). The Sesia-Lanzo Zone: A slice of continental crust, with alpine HP-LT assemblages in the Western Italian Alps. *Rendiconti*

- della Società Italiana di Mineralogia e Petrologia, 33, 281–334.
- Dal Piaz, G. V., Hunziker, J. C., & Martinotti, G. (1972). La zona Sesia-Lanzo e l'evoluzione tettonico-metamorfica delle Alpi nordoccidentali interne. *Memorie della Società Geologica Italiana*, 11, 433–466.
- Delleani, F., Spalla, M. I., Castelli, D., & Gosso, G. (2012). Multiscale structural analysis in the subducted continental crust of the internal Sesia-Lanzo Zone (Monte Mucrone, Western Alps). *Journal of the Virtual Explorer*, 41(7), 1–35. doi:10.3809/jvirtex.2011.00287
- Delleani, F., Spalla, M. I., Castelli, D., & Gosso, G. (2013). A new petro-structural map of the Monte Mucrone metagranitoids (Sesia-Lanzo Zone, Western Alps). *Journal of Maps*, 9(3), 410–424. doi:10.1080/17445647.2013.800004
- Giuntoli, F., & Engi, M. (2016). Internal geometry of the central Sesia zone (Aosta Valley, Italy): HP tectonic assembly of continental slices. *Swiss Journal of Geosciences*, 109(3), 445–471. doi:10.1007/s00015-016-0225-4
- Gosso, G. (1977). Metamorphic evolution and fold history in the eclogite micaschists of the upper Gressoney valley (Sesia-Lanzo Zone, Western Alps). *Rendiconti della Società Italiana di Mineralogia e Petrologia*, 33, 389–407.
- Gosso, G., Messiga, B., Rebay, G., & Spalla, M. I. (2010). Interplay between deformation and metamorphism during eclogitization of amphibolites in the Sesia-Lanzo Zone of the Western Alps. *International Geology Review*, 52(10), 1193–1219. doi:10.1080/00206810903529646
- Gosso, G., Rebay, G., Roda, M., Spalla, M. I., Tarallo, M., Zanoni, D., & Zucali, M. (2015). Taking advantage of petrostructural heterogeneities in subduction-collisional orogens, and effect on the scale of analysis. *Periodico di Mineralogia* (2015), 84(3B), 779–825. doi:10.2451/2015PM0452
- Handy, M. R., Babist, J., Wagner, R., Rosenberg, C. L., & Konrad, M. (2005). Decoupling and its relations to strain partitioning in continental lithosphere: Insight from the periadriatic fault system (European Alps). *Geological Society, London, Special Publications*, 243(1), 249–276.
- Kapferer, N., Mercolli, I., Berger, A., Ovtcharova, M., & Fügenschuh, B. (2012). Dating emplacement and evolution of the orogenic magmatism in the internal western Alps: 2. The Biella Volcanic Suite. *Swiss Journal of Geosciences*, 105, 67–84. doi:10.1007/s00015-012-0092-6
- Kretz, R. (1983). Symbols for rock-forming minerals. *American Mineralogist*, 68, 277–279.
- Lardeaux, J. M. (2014). Deciphering orogeny: A metamorphic perspective. Examples from European Alpine and Variscan belts part I: Alpine metamorphism in the Western Alps. A review. *Bulletin de la Société Géologique de France*, 185(2), 93–114.
- Lardeaux, J. M., Gosso, G., Kiénast, J. R., & Lombardo, B. (1982). Relations entre le métamorphisme et la déformation dans la zone Sesia-Lanzo (Alpes Occidentales) et le problème de l'eclogitisation de la croûte continentale. *Bulletin de la Société Géologique de France*, S7-XXIV(7), 793–800.
- Lardeaux, J. M., & Spalla, M. I. (1990). Tectonic significance of P-T-t paths in metamorphic rocks: Examples from ancient and modern orogenic belts. *Memorie della Società Geologica Italiana*, 45, 51–69.
- Lardeaux, J. M., & Spalla, M. I. (1991). From granulites to eclogites in the Sesia zone (Italian Western Alps): A record of the opening and closure of the Piedmont ocean. *Journal of Metamorphic Geology*, 9, 35–59.
- Manzotti, P., Ballèvre, M., Zucali, M., Robyr, M., & Engi, M. (2014). The tectonometamorphic evolution of the Sesia-Dent Blanche nappes (Internal Western Alps): Review and synthesis. *Swiss Journal of Geosciences*, 107, 309–336. doi:10.1007/s00015-014-0172-x
- Mørk, M. B. (1985). A gabbro eclogite transition of Flemsoy, Suamore, western Norway. *Chemical Geology*, 50, 283–310. doi:10.1016/0009-2541(85)90125-1
- Myers, J. S. (1970). Gneiss types and their significance in the repeatedly deformed and metamorphosed Lewisian complex of Western Harris, Outer Hebrides. *Scottish Journal of Geology*, 6, 186–199. doi:10.1144/sjg06020186
- Passchier, C. W., Myers, J. S., & Kroner, A. (1990). *Field geology of high-grade gneiss terrains*. Berlin Heidelberg: Springer-Verlag.
- Passchier, C. W., Urai, J. L., Van Loon, J., & Williams, P. F. (1981). Structural geology of the central Sesia Lanzo Zone. *Geologie en Mijnbouw*, 60, 497–507.
- Pognante, U. (1989). Lawsonite, blueschist and eclogite formation in the southern Sesia Zone (Western Alps, Italy). *European Journal of Mineralogy*, 1, 89–104.
- Pognante, U. (1991). Petrological constraints on the eclogite- and blueschist-facies metamorphism and P-T-t paths in the Western Alps. *Journal of Metamorphic Geology*, 9(1), 5–17. doi:10.1111/j.1525-1314.1991.tb00501.x
- Pognante, U., Compagnoni, R., & Gosso, G. (1980). Micro-mesostructural relationships in the continental eclogitic rocks of the Sesia-Lanzo Zone: A record of a subduction cycle (Italian Western Alps). *Rendiconti della Società Italiana di Mineralogia e Petrologia*, 36, 169–186.
- Pognante, U., Talarico, F., Rastelli, N., & Ferrati, N. (1987). High pressure metamorphism in the nappes of the Valle dell'Orco traverse (Western Alps Collisional Belt). *Journal of Metamorphic Geology*, 5, 397–414.
- Polino, R., Dal Piaz, G. V., & Gosso, G. (1990). Tectonic erosion at the Adria margin and accretionary processes for the Cretaceous orogeny of the Alps. *Mémoires de la Société géologique de France*, 156, 345–367.
- Ramsbotham, W., Inger, S., Cliff, B., Rex, D., & Barnicoat, A. (1994). Time constraints on the metamorphic and structural evolution of the southern Sesia-Lanzo Zone, Western Italian Alps. *Mineralogical Magazine*, 58A, 758–759.
- Regis, D., Rubatto, D., Darling, J., Cenko-Tok, B., Zucali, M., & Engi, M. (2014). Multiple metamorphic stages within an eclogite facies terrane (Sesia Zone, Western Alps) revealed by U/Th-Pb petrochronology. *Journal of Petrology*, 55(7), 1429–1456. doi:10.1093/petrology/egu029
- Roda, M., Spalla, M. I., & Marotta, A. M. (2012). Integration of natural data within a numerical model of ablative subduction: A possible interpretation for the Alpine dynamics of the Austroalpine crust. *Journal of Metamorphic Geology*, 30, 973–996. doi:10.1111/jmg.12000
- Roda, M., & Zucali, M. (2008). Meso and microstructural evolution of the Mont Morion metaintrusive complex (Dent Blanche nappe, Austroalpine domain, Valpelline, Western Italian Alps). *Bollettino della Società Geologica Italiana*, 127, 105–123.
- Romer, R. L., Schärer, U., & Steck, A. (1996). Alpine and pre-Alpine magmatism in the root-zone of the Western Central Alps. *Contributions to Mineralogy and Petrology*, 123, 138–158.
- Rubatto, D., Regis, D., Hermann, J., Boston, K., Engi, M., Beltrando, M., & McAlpine, S. R. B. (2011). Yo-yo subduction recorded by accessory minerals in the Italian Western Alps. *Nature Geoscience*, 4, 338–342. doi:10.1038/NGEO1124

- Salvi, F., Spalla, M. I., Zucali, M., & Gosso, G. (2010). Three-dimensional evaluation of fabric evolution and metamorphic reaction progress in polycyclic and polymetamorphic terrains: A case from the Central Italian Alps. *Geological Society, London, Special Publications*, 332, 173–187. doi:10.1144/SP332.11
- Spalla, M. I., De Maria, L., Gosso, G., Miletto, M., & Pognante, U. (1983). Deformazione e metamorfismo della Zona Sesia-Lanzo meridionale al contatto con la falda piemontese e con il massiccio di Lanzo, Alpi Occidentali. *Memorie della Società Geologica Italiana*, 26, 499–514.
- Spalla, M. I., Gosso, G., Marotta, A. M., Zucali, M., & Salvi, F. (2010). Analysis of natural tectonic systems coupled with numerical modelling of the polycyclic continental lithosphere of the Alps. *International Geology Review*, 52(10–12), 1268–1302. doi:10.1080/00206814.2010.482737
- Spalla, M. I., Lardeaux, J. M., Dal Piaz, G. V., & Gosso, G. (1991). Metamorphisme et tectonique a la marge externe de la zone Sesia-Lanzo (Alpes Occidentales). *Memorie della Società Geologica Italiana*, 43, 361–369.
- Spalla, M. I., Lardeaux, J. M., Dal Piaz, G. V., Gosso, G., & Messiga, B. (1996). Tectonic significance of Alpine eclogites. *Journal of Geodynamics*, 21, 257–285.
- Spalla, M. I., Siletto, G. B., di Paola, S., & Gosso, G. (2000). The role of structural and metamorphic memory in the distinction of tectonometamorphic units, the basement of the Como Lake in the Southern Alps. *Journal of Geodynamics*, 30, 191–204.
- Spalla, M. I., Zucali, M., di Paola, S., & Gosso, G. (2005). A critical assessment of tectono-thermal memory of rocks and definition of tectonometamorphic units: Evidence from fabric and degree of metamorphic transformation. *Geological Society, London, Special Publications*, 243(1), 227–247.
- Spalla, M. I., & Zulbati, F. (2003). Structural and petrographic map of the southern Sesia-Lanzo Zone (Monte Soglio – Rocca Canavese, Western Alps, Italy). *Memorie di Scienze Geologiche Padova*, 55, 119–127.
- Stünitz, H. (1991). Folding and shear deformation in quartzites, inferred from crystallographic preferred orientation and shape fabrics. *Journal of Structural Geology*, 13(1), 71–86.
- Tropper, P., & Essene, E. J. (2002). Thermobarometry in eclogites with multiple stages of mineral growth: An example from the Sesia-Lanzo Zone (Western Alps, Italy). *Schweizerische Mineralogische und Petrographische Mitteilungen*, 82(3), 487–514. doi:10.5169/seals-62377
- Venturini, G. (1995). Geology, geochemistry and geochronology of the inner central Sesia Zone (Western Alps, Italy). *Mémoires de Géologie (Lausanne)*, 25, 1–143.
- Venturini, G., Martinotti, G., Armando, G., Barbero, M., & Hunziker, J. C. (1994). The Central Sesia Lanzo Zone (Western Italian Alps): New field observations and lithostratigraphic subdivisions. *Schweizerische Mineralogische und Petrographische Mitteilungen*, 74, 115–125.
- Zanoni, D. (2016). Structure and petrography of the Southwestern margin of the Biella pluton, Western Alps. *Journal of Maps*, 12(3), 597–620. doi:10.1080/17445647.2015.1056259
- Zanoni, D., Bado, L., Spalla, M. I., Zucali, M., & Gosso, G. (2008). Structural analysis of the Northeastern margin of the tertiary intrusive stock of Biella (Western Alps, Italy). *Bollettino della Società Geologica Italiana [Italian Journal of Geoscience]*, 127, 125–140.
- Zanoni, D., Spalla, M. I., & Gosso, G. (2010). Structure and PT estimates across late collisional plutons: Constraints on the exhumation of western Alpine continental HP units. *International Geology Review*, 52(10–12), 1244–1267. doi:10.1080/00206814.2010.482357
- Zucali, M. (2011). Coronitic microstructures in patchy eclogitised continental crust: The Lago della Vecchia pre-Alpine metagranite (Sesia-Lanzo Zone, Western Italian Alps). *Journal of the Virtual Explorer, Electronic Edition*, 38, 3–28. doi:10.3809/jvirtex.2011.00286
- Zucali, M., & Spalla, M. I. (2011). Prograde lawsonite during the flow of continental crust in the Alpine subduction: Strain vs metamorphism partitioning, a field-analysis approach to infer tectono metamorphic evolutions (Sesia-Lanzo Zone, Western Italian Alps). *Journal of Structural Geology*, 33, 381–398. doi:10.1016/j.jsg.2010.12.006
- Zucali, M., Spalla, M. I., & Gosso, G. (2002). Strain partitioning and fabric evolution as a correlation tool: The example of the Eclogitic Micaschists complex in the Sesia-Lanzo Zone (Monte Mucrone-Monte Mars, Western Alps, Italy). *Schweizerische Mineralogische und Petrographische Mitteilungen*, 82, 429–454.